SUPPLEMENTARY DATA

The Synaptonemal Complex Central Region Modulates Crossover Pathways and Feedback Control of Meiotic Double-Strand Break Formation

Min-Su Lee, Mika T. Higashide, Hyungseok Choi, Ke Li, Soogil Hong, Kangseok Lee, Akira Shinohara, Miki Shinohara, Keun P. Kim

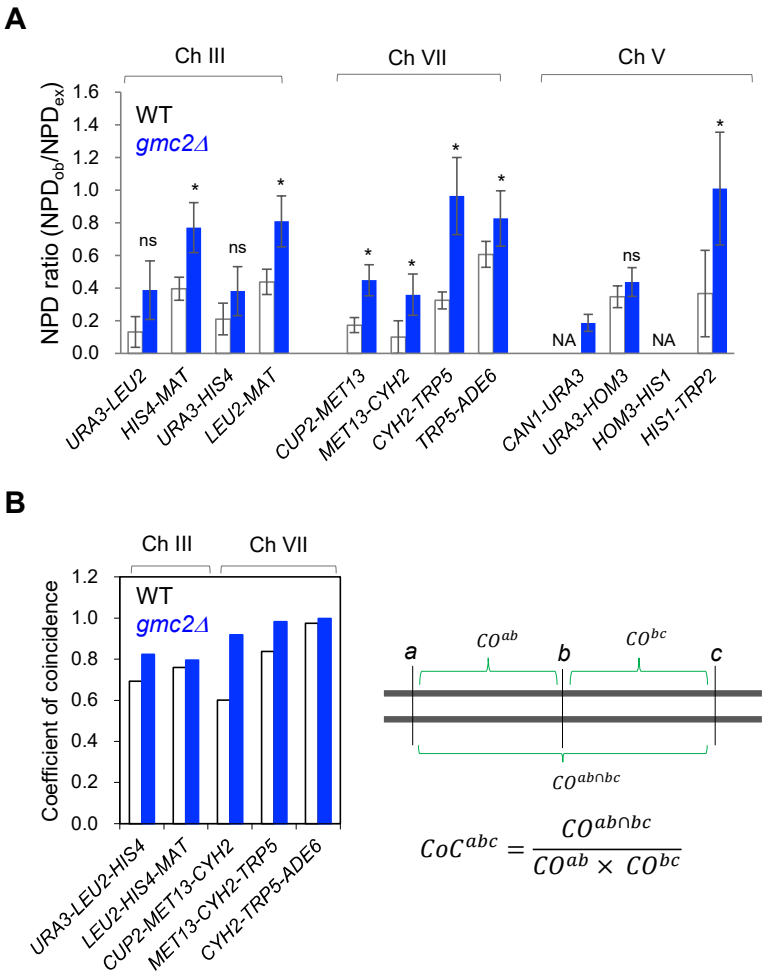

Supplementary Figure S1. NPD ratio and coefficient of coincidence.

(A) CO interference in NPD ratio in chromosomes III, VII, and V.

(B) Coefficient of coincidence in chromosomes III and VII.

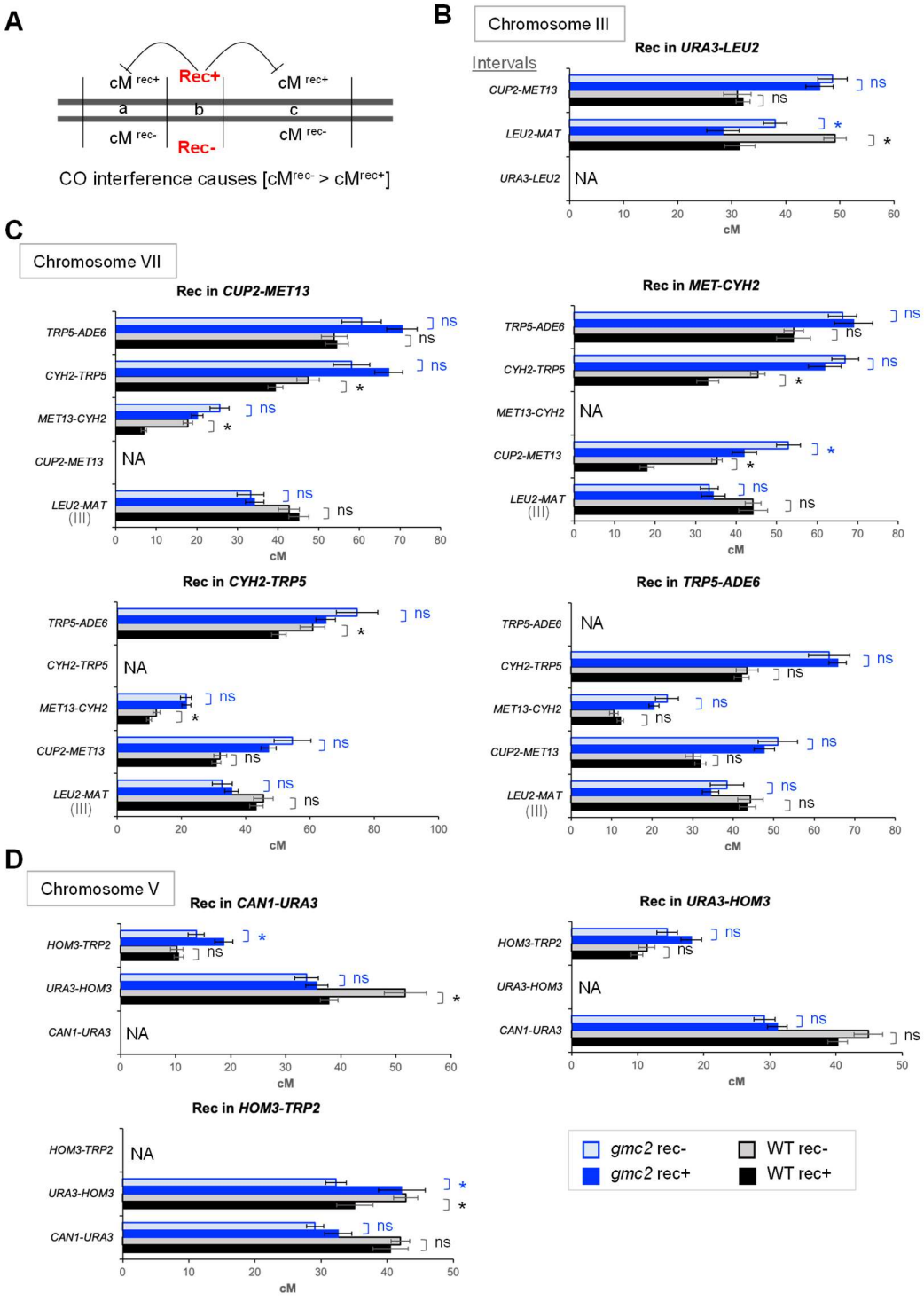

Supplementary Figure S2. **Inter-interval interference in WT and *gmc2Δ* cells.**

Tetrad data shown in Figure 1 were analyzed by the Malkova method (58). (A) Schematic diagram for the analysis. (B) CO frequencies (cM) of the next interval, *LEU2-MAT*, and an independent interval, *CUP2-MET13*, on chromosome VII after rec+ or rec– categorization of the *URA3-LEU2* in chromosome III. (C) CO frequencies (cM) after rec+ or rec– categorization of each indicated interval on chromosome VII, and (D) chromosome V. Statistical significances were determined by testing whether 2(S.E.[cM^{rec-}-cM^{rec+}]) < |cM^{rec-}-cM^{rec+}|. Asterisks, significant difference; ns, not-significant; NA,

not assigned.

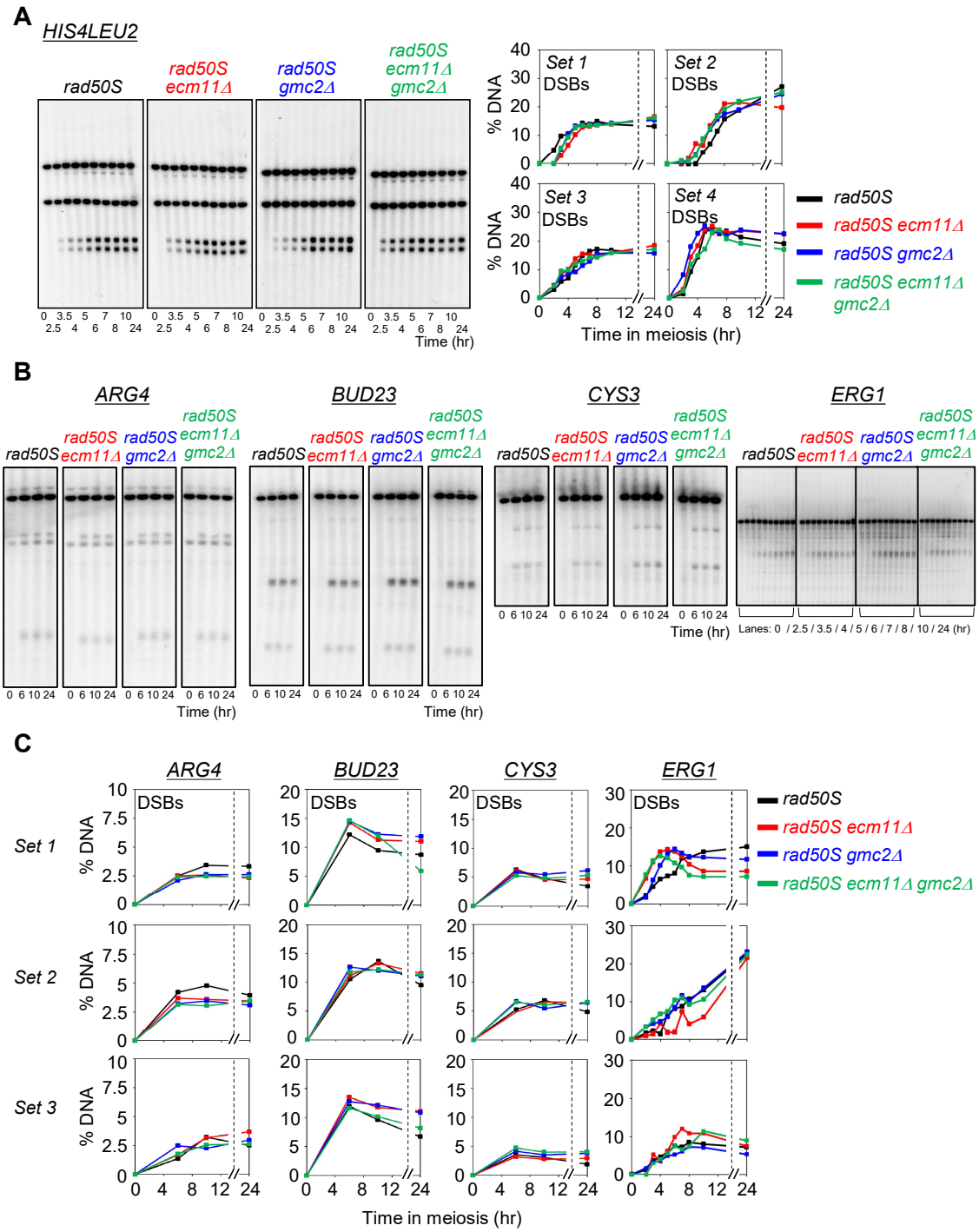

Supplementary Figure S3. Analysis of DSB levels in a *rad50S* background.

(A) Gel analysis (1D) at *HIS4LEU2* locus in *rad50S, rad50S ecm11Δ*, *rad50S gmc2Δ*, and *rad50S ecm11Δ gmc2Δ* cells (left). Quantification of DSBs from three independent meiotic cultures (right).

(B) Gel analysis (1D) at different loci in *rad50S, rad50S ecm11Δ, rad50S gmc2Δ*, and *rad50S ecm11Δ gmc2Δ* strains. *ARG4*, *BUD23, CYS3,* and *ERG1* loci located on chromosomes VIII, III, I, and VII, respectively.

(C) Quantitative analysis of DSBs at various loci in three sets of independent meiotic cultures.

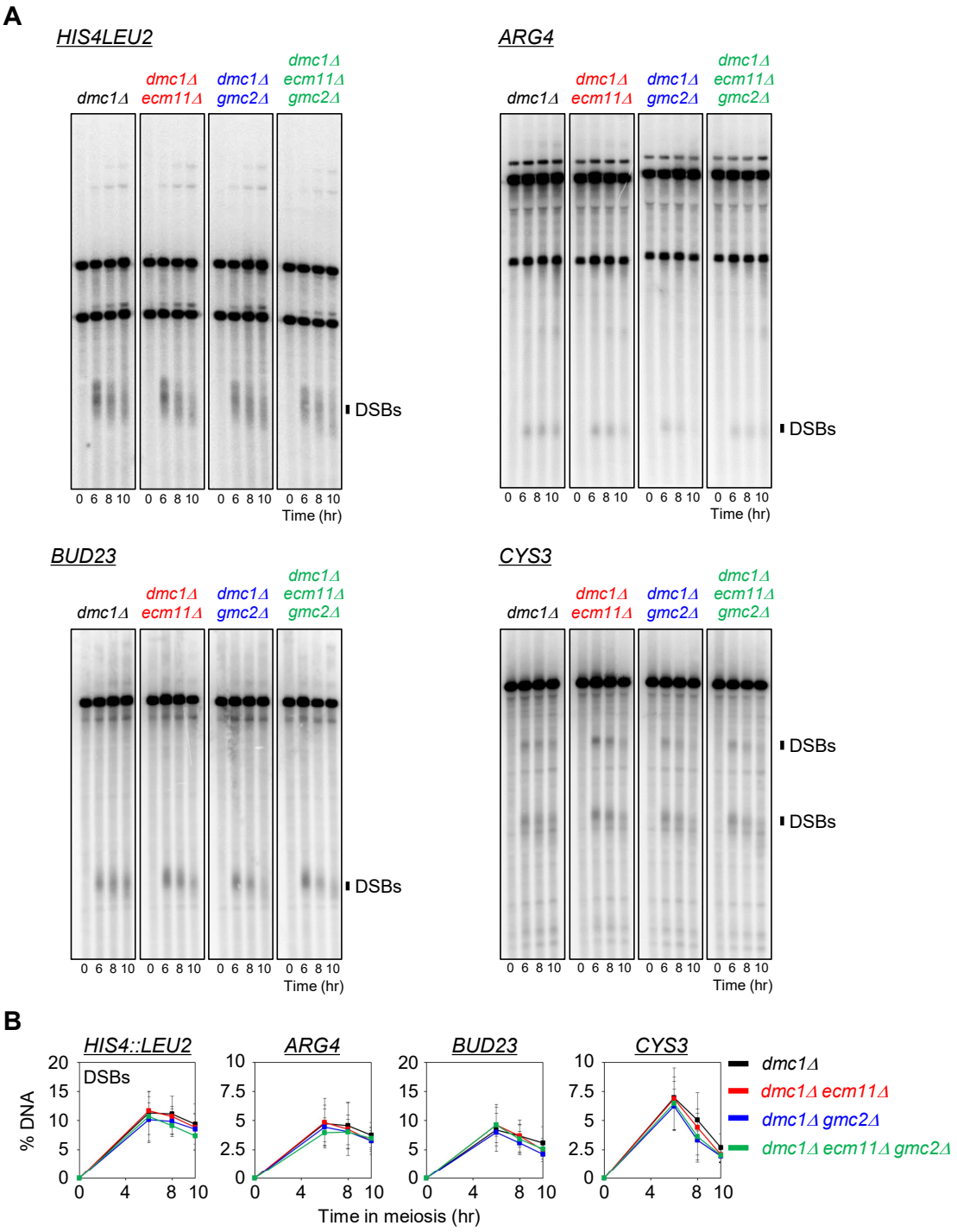

Supplementary Figure S4. Analysis of DSB levels in a *dmc1Δ* background.

(A) Gel analysis (1D) at the *HIS4LEU2*, *ARG4*, *BUD23,* and *CYS3* loci in *dmc1Δ*, *dmc1Δ ecm11Δ*, *dmc1Δ gmc2Δ*, and *dmc1Δ ecm11Δ gmc2Δ* mutants.

(B) Quantification of DSBs. Data are the means ± SD (N = 3).

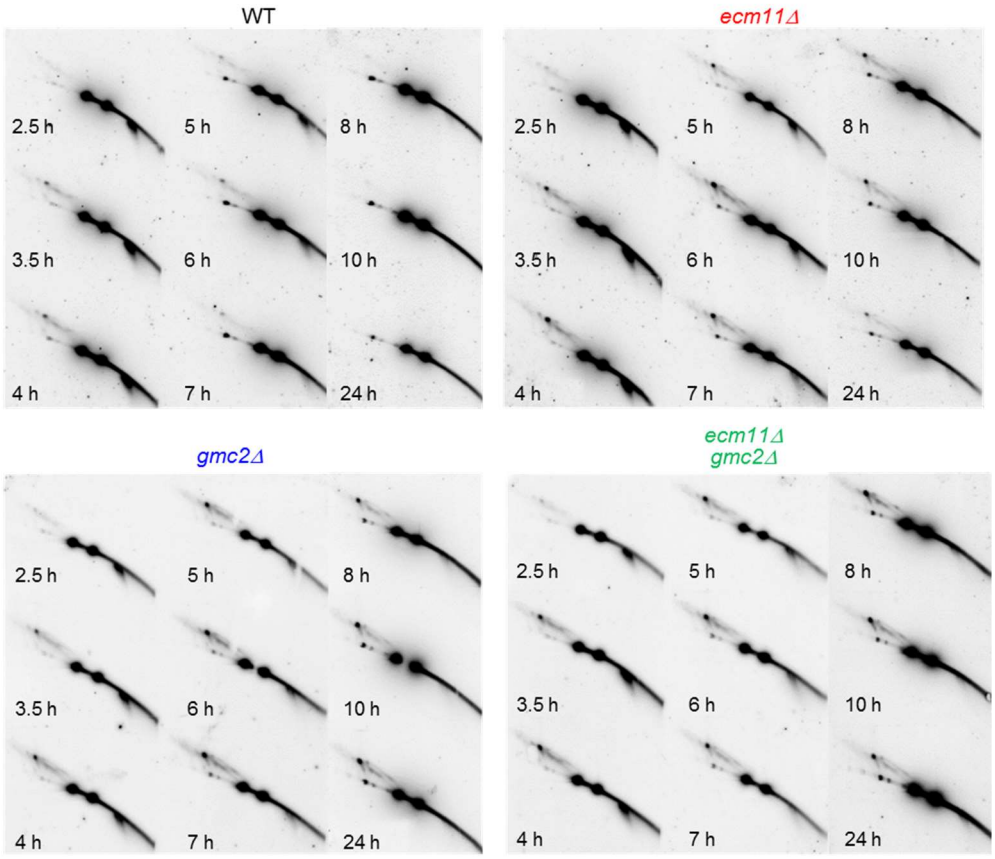

Supplementary Figure S5. Two-dimensional gel analysis for WT, *ecm11Δ*, *gmc2Δ*, and *ecm11Δ gmc2Δ* cells at the *HIS4LEU2* hotspot.

Two-dimensional gel images of Southern blotting for WT, *ecm11Δ*, *gmc2Δ*, and *ecm11Δ gmc2Δ* cells at the *HIS4LEU2* locus. Images show DNA species from representative meiotic time courses.

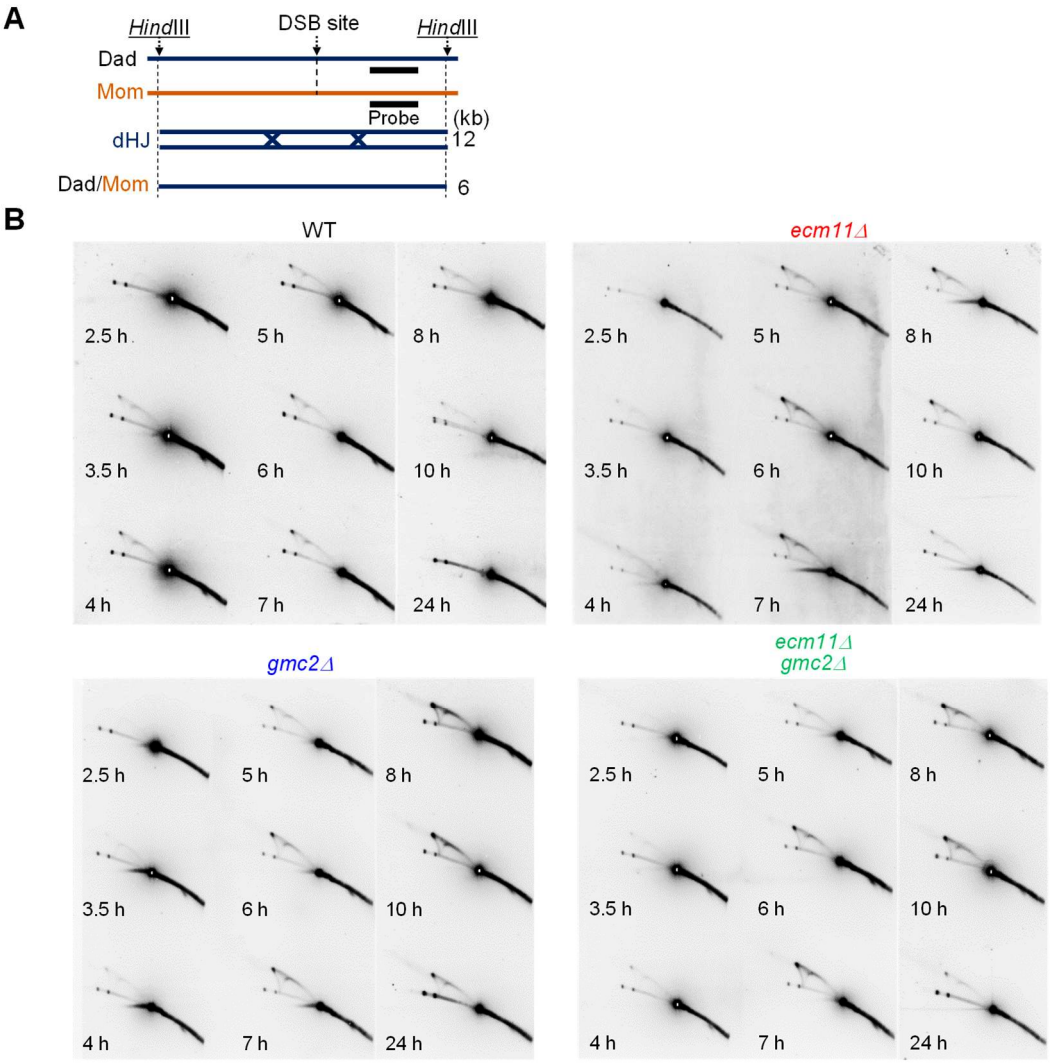

Supplementary Figure S6. Two-dimensional gel analysis for WT, *ecm11Δ*, *gmc2Δ*, and *ecm11Δ gmc2Δ* cells at the *ERG1* locus.

(A) Physical map of the *ERG1* locus.

(B) Two-dimensional gel images of Southern blotting for WT, *ecm11Δ*, *gmc2Δ*, and *ecm11Δ gmc2Δ* cells at the *ERG1* locus. Images show DNA species from representative meiotic time courses.

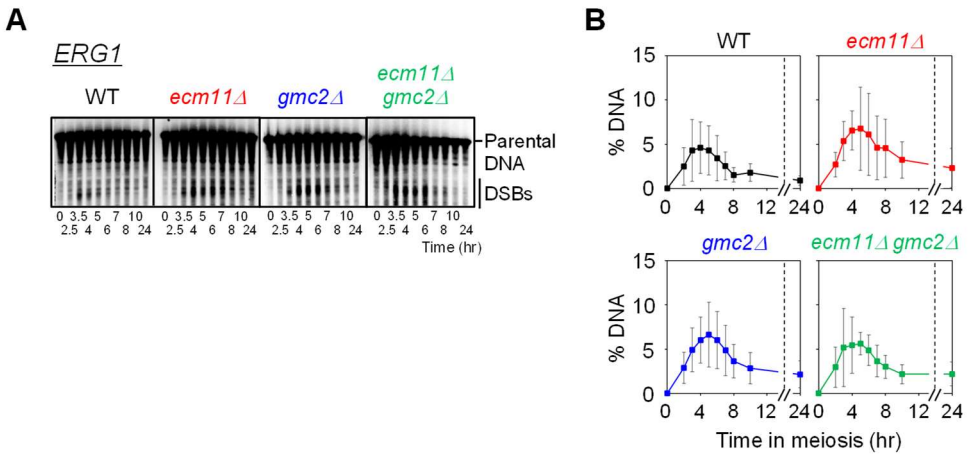

Supplementary Figure S7. Analysis of DSB levels in WT, *ecm11Δ*, *gmc2Δ*, and *ecm11Δ gmc2Δ* cells at the *ERG1* locus.

(A) Representative 1D gel images of WT, *ecm11Δ*, *gmc2Δ*, and *ecm11Δ gmc2Δ* at the *ERG1* locus.

(B) Quantitative analysis of images shown in (A). Error bars indicate the means ± SD (N = 3).

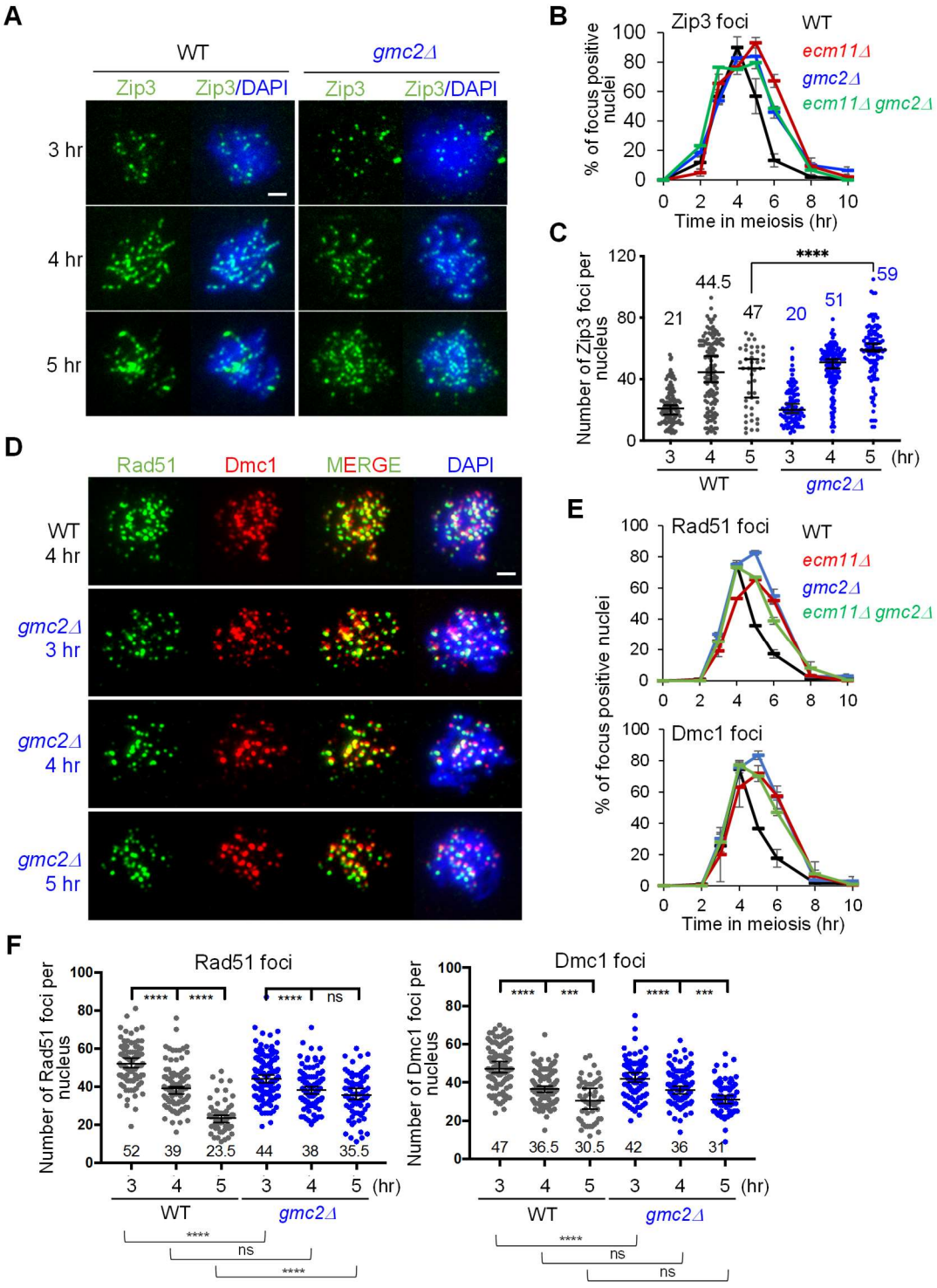

Supplementary Figure S8. Chromosome analysis of WT, *ecm11Δ*, *gmc2Δ*, and *ecm11Δ gmc2Δ* cells.

(A) Representative images of chromosome spreads immunostained for Zip3 (green) along meiotic progression of WT and *gmc2Δ* cells.

(B) Quantification of the number of Zip3 foci-positive nuclei along meiotic progression in WT (black), *ecm11Δ* (red), *gmc2Δ* (blue), and *ecm11Δ gmc2Δ* (green) cells.

(C) Quantification of the number of Zip3 foci along meiotic progression in WT and *gmc2Δ* cells.
(D) Representative images of chromosome spreads and cells immunostained for Rad51 (green) and Dmc1 (red) along meiotic progression in WT and mutant cells.
(E) Quantification of the number of Rad51 and Dmc1 foci-positive nuclei along meiotic progression.
(F) Quantification of the number of Rad51 and Dmc1 foci along meiotic progression. Error bars indicate the median and 95% C.I., statistical significance was analyzed through the Mann-Whitney *U*-test (**** $P < 0.0001$, *** $P < 0.001$ and ns indicates $P > 0.05$).

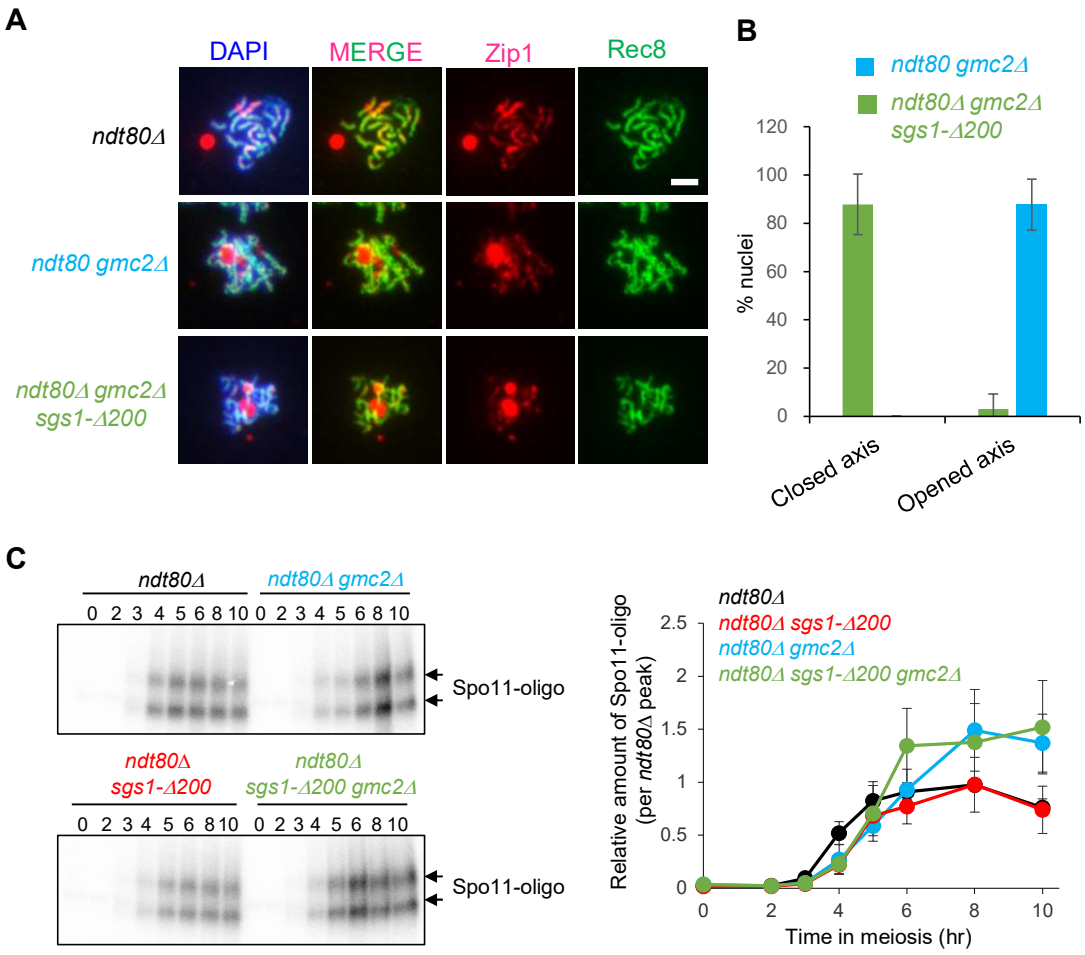

Supplementary Figure S9. EG complex prevents additional DSB formation after the Ndt80 pathway, even with pseudo-synapsis.

(A) Representative image of meiotic nuclear spread from *ndt80Δ gmc2Δ*, and *ndt80Δ gmc2Δ sgs1-Δ200* cells at 8 h post-meiosis entry. Cells were co-stained for anti-Rec8 (green), anti-Zip1 (red), and DAPI (blue).

(B) Analysis of the chromosome axis.

(C) Representative image of ^{32}P-labeled DNA fragments covalently bound to Spo11-3FLAG in immunoprecipitates and quantitative analysis of the images for *ndt80Δ*, *ndt80Δ gmc2Δ*, *ndt80Δ sgs1-Δ200*, and *ndt80Δ gmc2Δ sgs1-Δ200* mutants. Error bars indicate the means ± SD (*N* = 4).

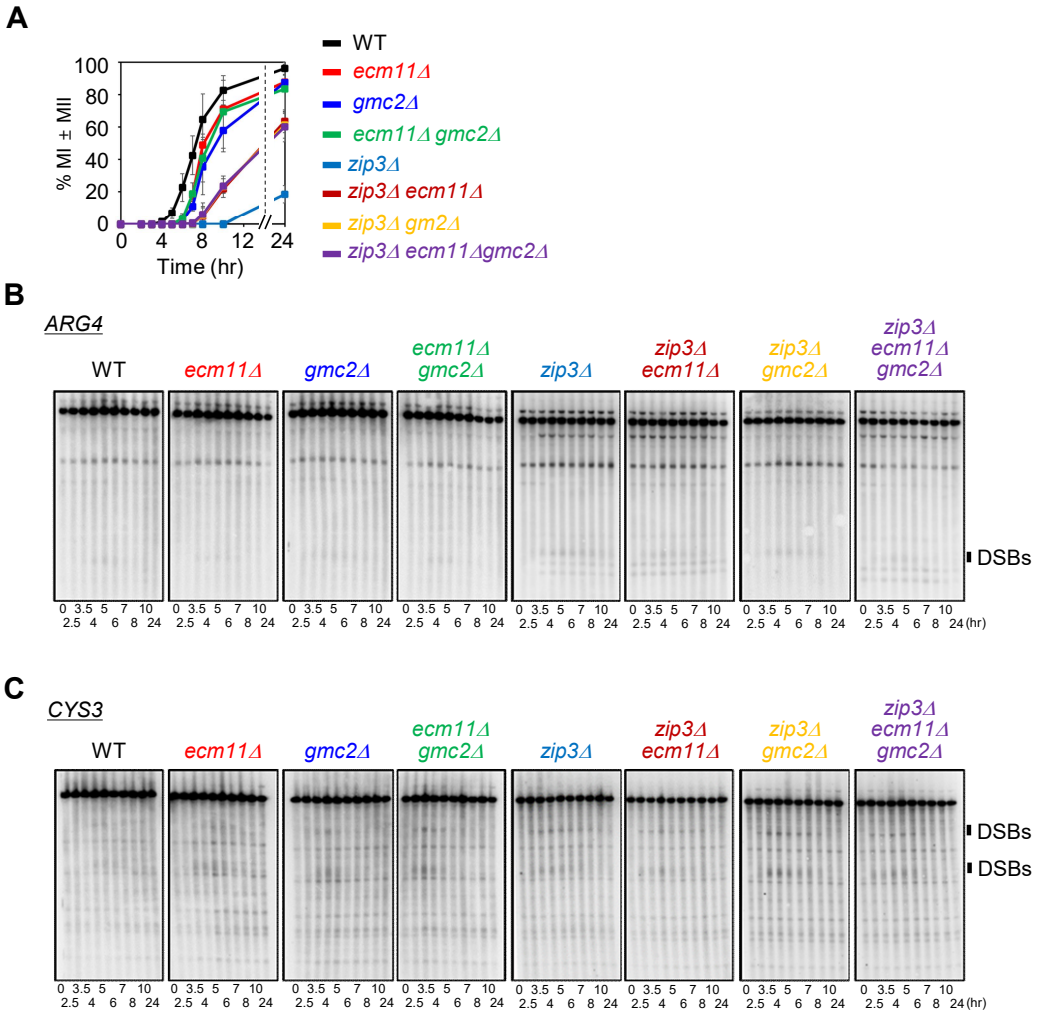

Supplementary Figure S10. Absence of the EG complex restrains *zip3Δ*-induced additional DSBs at various loci.

(A) Meiotic division for *zip3Δ*, *zip3Δ ecm11Δ*, *zip3Δ gmc2Δ*, and *zip3Δ ecm11Δ gmc2Δ* mutants. Error bars indicate the means ± SD (N = 3).

(B and C) Southern blot analysis (1D) of *ARG4* and *CYS3* loci in *zip3Δ*, *zip3Δ ecm11Δ*, *zip3Δ gmc2Δ*, and *zip3Δ ecm11Δ gmc2Δ* mutants.

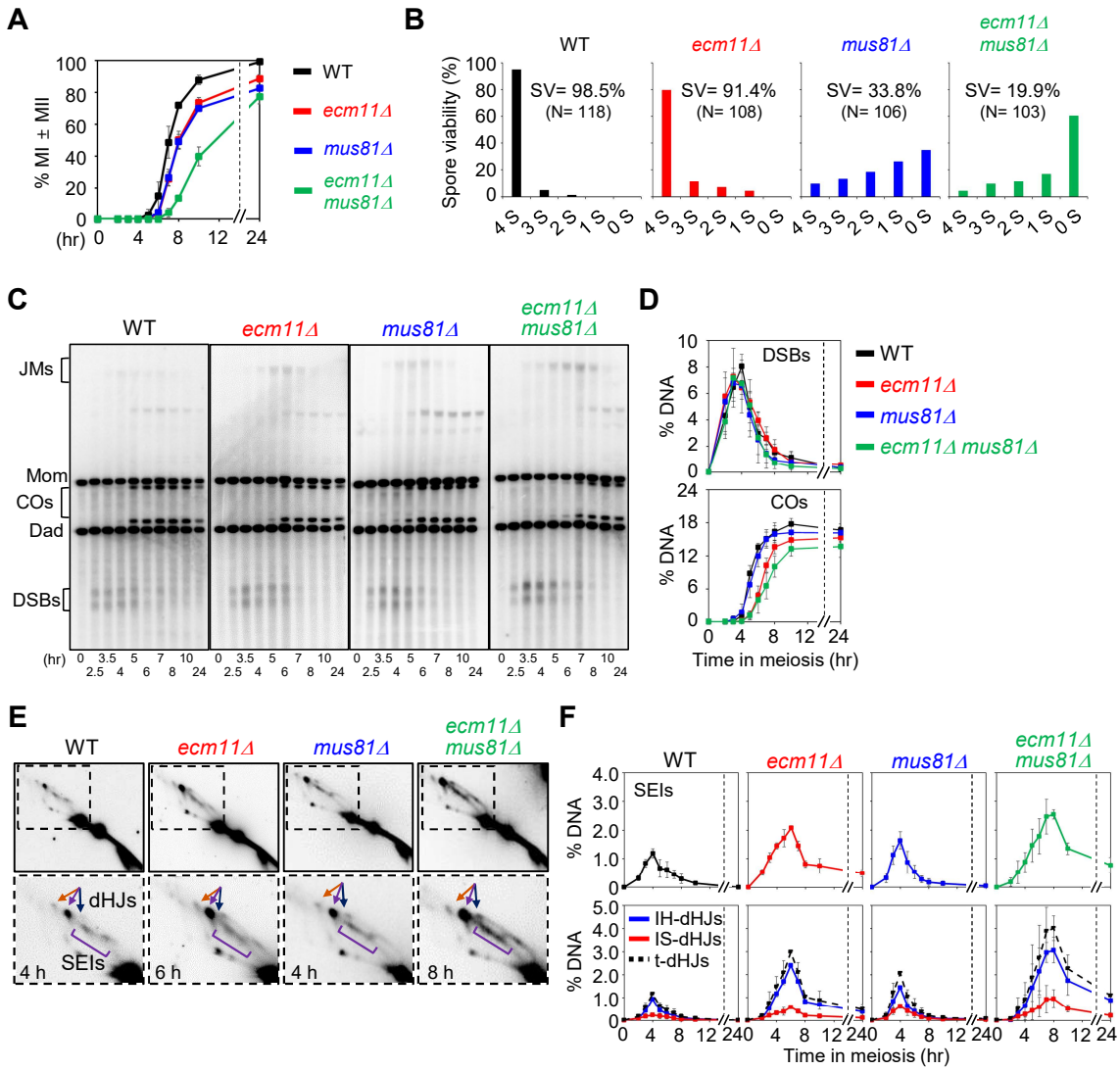

Supplementary Figure S11. The EG complex functions independently from Mus81-Mms4 in meiotic recombination.

(A) Meiotic nuclear division of WT, *ecm11Δ*, *mus81Δ*, and *ecm11Δ mus81Δ* strains. Error bars indicate the means ± SD (N = 3).

(B) Analysis of spore viability of WT, *ecm11Δ*, *mus81Δ*, and *ecm11Δ mus81Δ* strains.

(C) 1D gel analysis of WT, *ecm11Δ*, *mus81Δ*, and *ecm11Δ mus81Δ* cells.

(D) Quantification of DSBs and COs. The plots for WT and *ecm11Δ* are from Figure 2D. Error bars indicate the means ± SD (N = 3).

(E) 2D gel analysis of WT, *ecm11Δ*, *mus81Δ*, and *ecm11Δ mus81Δ* cells. The gel images for WT and *ecm11Δ* are from Figure 3B.

(F) Quantification of SEIs and dHJs. The plots for WT and *ecm11Δ* are from Figure 3B. Error bars indicate the means ± SD (N = 3).

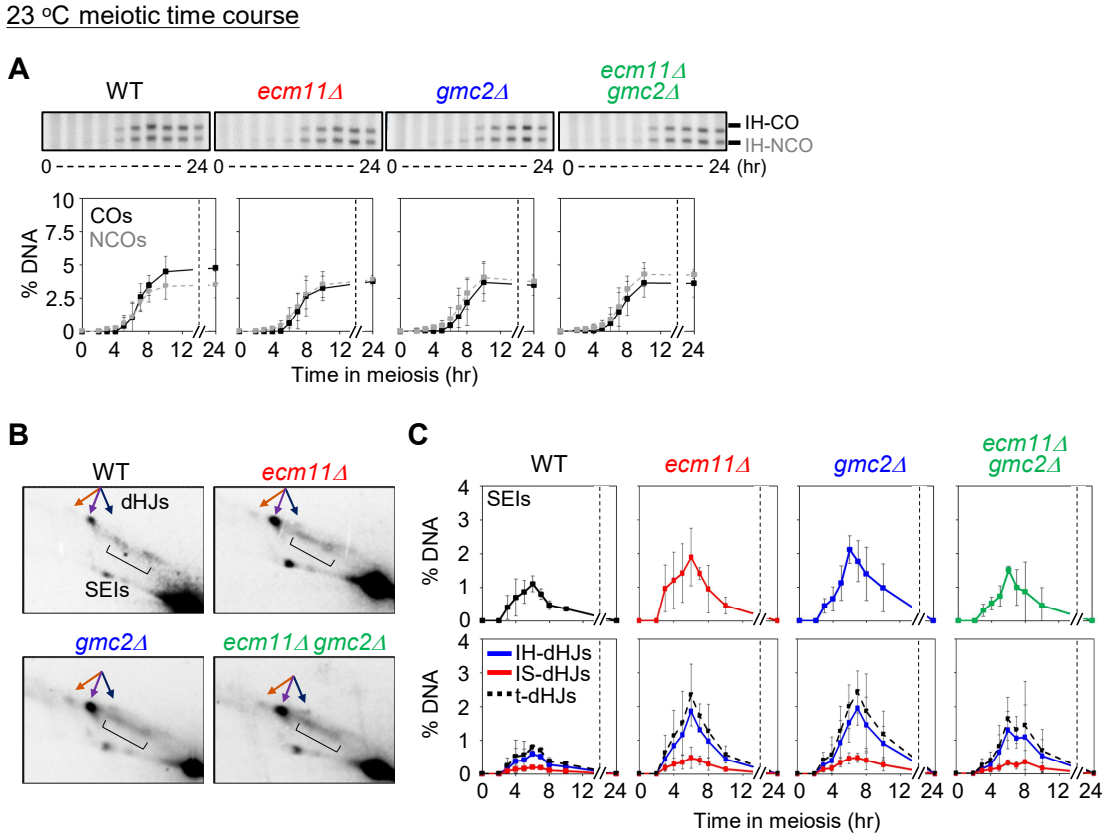

Supplementary Figure S12. Meiotic recombination of WT, *ecm11Δ*, *gmc2Δ*, and *ecm11Δ gmc2Δ* cells at low temperature.

(A) CO/NCO analysis of WT, *ecm11Δ*, *gmc2Δ*, and *ecm11Δ gmc2Δ* cells at low temperature (23 °C). Error bars indicate the means ± SD (N = 3).

(B) Representative images of two-dimensional gel analysis.

(C) Quantitative analysis of results shown in panel B. Error bars indicate the means ± SD (N = 3).

Supplementary table 1. Yeast strains used in this study.

Strain	Genotype†
KKY276	*MATa/MATα HIS4::LEU2-(BamHI)/his4-x::LEU2-(NgoMIV)-URA3*
KKY730	*MATa/MATα HIS4::LEU2-(BamHI)/his4-x::LEU2-(NgoMIV)-URA3, ecm11Δ::HygB/"*
KKY732	*MATa/MATα HIS4::LEU2-(BamHI)/his4-x::LEU2-(NgoMIV)-URA3, gmc2Δ::KanMX/"*
KKY855	*MATa/MATα HIS4::LEU2-(BamHI)/his4-x::LEU2-(NgoMIV)-URA3, ecm11Δ::HygB/", gmc2Δ::KanMX/"*
KKY885	*MATa/MATα HIS4::LEU2-(BamHI)/his4-x::LEU2-(NgoMIV)-URA3, rad50S::URA3/"*
KKY984	*MATa/MATα HIS4::LEU2-(BamHI)/his4-x::LEU2-(NgoMIV)-URA3, rad50s::URA3/", ecm11Δ::HygB/"*
KKY983	*MATa/MATα HIS4::LEU2-(BamHI)/his4-x::LEU2-(NgoMIV)-URA3, rad50s::URA3, gmc2Δ::KanMX/"*
KKY985	*MATa/MATα HIS4::LEU2-(BamHI)/his4-x::LEU2-(NgoMIV)-URA3, rad50s::URA3/", ecm11Δ::HygB/", gmc2Δ::KanMX/"*
KKY389	*MATa/MATα HIS4::LEU2-(BamHI)/his4-x::LEU2-(NgoMIV)-URA3, ndt80Δ::KanMX4/"*
KKY1469	*MATa/MATα HIS4::LEU2-(BamHI)/his4-x::LEU2-(NgoMIV)-URA3, ndt80Δ::KanMX4/", ecm11Δ::HygB/"*
KKY1471	*MATa/MATα HIS4::LEU2-(BamHI)/his4-x::LEU2-(NgoMIV)-URA3, ndt80Δ::KanMX4/", gmc2Δ::KanMX/"*
KKY1473	*MATa/MATα HIS4::LEU2-(BamHI)/his4-x::LEU2-(NgoMIV)-URA3, ndt80Δ::KanMX4/", ecm11Δ::HygB/", gmc2Δ::KanMX/"*
KKY2945	*MATa/MATα HIS4::LEU2-(BamHI)/his4-x::LEU2-(NgoMIV)-URA3, ERG1::SalI / ERG1::SpeI*
KKY3012	*MATa/MATα HIS4::LEU2-(BamHI)/his4-x::LEU2-(NgoMIV)-URA3, ERG1::SalI / ERG1::SpeI, ecm11Δ::HygB/"*
KKY2996	*MATa/MATα HIS4::LEU2-(BamHI)/his4-x::LEU2-(NgoMIV)-URA3, ERG1::SpeI / ERG1::SalI, gmc2Δ::KanMX/"*
KKY2997	*MATa/MATα HIS4::LEU2-(BamHI)/his4-x::LEU2-(NgoMIV)-URA3, ERG1::SpeI / ERG1::SalI, ecm11Δ::HygB/", gmc2Δ::KanMX/"*
KKY1054	*MATa/MATα HIS4::LEU2-(BamHI)/his4-x::LEU2-(NgoMIV)-URA3, zip3Δ::KanMX/"*
KKY1060	*MATa/MATα HIS4::LEU2-(BamHI)/his4-x::LEU2-(NgoMIV)-URA3, zip3Δ::KanMX/", ecm11Δ::HygB/"*
KKY1115	*MATa/MATα HIS4::LEU2-(BamHI)/his4-x::LEU2-(NgoMIV)-URA3, zip3Δ::KanMX/", gmc2Δ::KanMX/"*
KKY1059	*MATa/MATα HIS4::LEU2-(BamHI)/his4-x::LEU2-(NgoMIV)-URA3, zip3Δ::KanMX/", ecm11Δ::HygB/", gmc2Δ::KanMX/"*
KKY1431	*MATa/MATα HIS4::LEU2-(BamHI)/his4-x::LEU2-(NgoMIV)-URA3, dmc1Δ::KanMX/"*
KKY1397	*MATa/MATα HIS4::LEU2-(BamHI)/his4-x::LEU2-(NgoMIV)-URA3, dmc1Δ::KanMX/", ecm11Δ::HygB/"*
KKY1400	*MATa/MATα HIS4::LEU2-(BamHI)/his4-x::LEU2-(NgoMIV)-URA3, dmc1Δ::KanMX/", gmc2Δ::KanMX/"*
KKY1399	*MATa/MATα HIS4::LEU2-(BamHI)/his4-x::LEU2-(NgoMIV)-URA3, dmc1Δ::KanMX/", ecm11Δ::HygB/", gmc2Δ::KanMX/"*

KKY6004	*MATa/MATα HIS4::LEU2-(BamHI+ori), his4-x::LEU2-(NgoMIV)--URA3, mus81Δ::KanMX/"*
KKY5992	*MATa/MATα HIS4::LEU2-(BamHI+ori), his4-x::LEU2-(NgoMIV)--URA3, ecm11Δ::HygB/", mus81Δ::KanMX/"*
MSY831	*MAT alpha, ho::LYS2, lys2, ura3, leu2::hisG, trp1::hisG*
MSY833	*MAT a, ho::LYS2, lys2, ura3, leu2::hisG, trp1::hisG*
MHY615	*MSY833/831 with SPO11-3FLAG::KanMX, ndt80Δ::LEU2*
MHY645	*MSY833/831 with SPO11-3FLAG::KanMX, ndt80Δ::LEU2, gmc2Δ::KanMX*
MSY5139	*MSY833/381 with ndt80Δ::LEU2*
MHY561	*MSY833/381 with ndt80Δ::LEU2, gmc2Δ::KanMX*
MHY812	*MSY833/831 with sgs1ΔC200::KanMX, ndt80Δ::LEU2, Spo11-3FLAG::KanMX*
MHY824	*MSY833/831 with sgs1ΔC200::KanMX, ndt80Δ::LEU2 gmc2Δ::KanMX, Spo11-3FLAG::KanMX*
MSY4988	*MAT alpha, ho::LYS2, lys2, HIS4-LEU2-URA3, ura3, leu2::hisG, cyh2-R, arg4-bgl*
MSY4304	*MAT a, ho::LYS2, lys2, his4B-leu2E, cup2-B, met13-B, trp5-S, ade6-B, arg4-bgl, ura3, leu2::hisG, arg4-bgl*
MSY4992	*gmc2Δ::KanMX, MSY4304*
MSY4990	*gmc2Δ::KanMX, MSY4988*
MSY5085	*MAT alpha, ura3, hom3-10, trp2, cyh2-R, his1, leu2::hisG (congenic SK1)*
S2921	*MAT a, ho::LYS2, lys2, can1R, leu2::hisG (congenic SK1)*
MSY5209	*gmc2Δ::HygB, MSY5085*
MSY5073	*gmc2Δ::HygB, S2921*

† All strains are isogenic derivatives of parental SK1.

Supplementary table 2. Genetic analysis of *gmc2Δ* cells by Papazian's NPD analysis on chromosomes III, V, and VII.

Chromosome III

Strain	Interval	PD [a]	TT	NPD_{obs}	Total	cM ± SE [b]	NPD_{exp}	NPD ratio ± SE [b]
Wild type	*URA3-LEU2*	919	352	2	1273	14.3 ± 0.70	15	0.13 ± 0.09
	LEU2-HIS4	1223	54	0	1277	2.1 ± 0.28	0.3	N.A.
	HIS4-MAT	491	808	49	1348	40.9 ± 1.5	124	0.40 ± 0.06
gmc2Δ	*URA3-LEU2*	764	297	5	1066	15.3 ± 0.91	13	0.39 ± 0.17
	LEU2-HIS4	1026	38	0	1064	1.8 ± 0.28	0.2	N.A.
	HIS4-MAT	563	518	36	1117	32.9 ± 1.6*	47	0.77 ± 0.14*

Chromosome VII

Strain	Intervals	PD [a]	TT	NPD_{obs}	Total	cM ± SE [b]	NPD_{exp}	NPD ratio ± SE [c]
Wild type	*CUP2-MET13*	539	686	15	1240	31.3 ± 1.1	87	0.17 ± 0.05
	MET13-CYH2	1005	296	1	1302	11.6 ± 0.6	10	0.10 ± 0.10
	CYH2-TRP5	455	844	48	1347	42.0 ± 1.5	148	0.32 ± 0.05
	TRP5-ADE6	381	847	97	1325	53.9 ± 2.0	160	0.61 ± 0.08
gmc2Δ	*CUP2-MET13*	284	597	54	932	48.4 ± 2.1*	114	0.45 ± 0.08*

	MET13-CYH2	624	383	9	1016	21.5 ± 1.1*	25	0.36 ± 0.12*
	CYH2-TRP5	226	740	110	1076	65.1 ± 2.5*	114	0.96 ± 0.13*
	TRP5-ADE6	244	686	119	1049	66.7 ± 2.7*	144	0.83 ± 0.12*

Chromosome V

Strain	Intervals	PD [a]	TT	NPD_{obs}	Total	cM ± SE [b]	NPD_{exp}	NPD ratio ± SE [b]
Wild type	*CAN1-URA3*	330	892	25	1247	41.8 ± 1.2	N.A. [c]	N.A.
	URA3-HIS1	425	760	46	1231	42.1 ± 1.6	127	0.36 ± 0.07
	HIS1-HOM3	1203	20	0	1223	0.82 ± 0.18	0.04	N.A.
	HOM3-TRP2	976	235	3	1214	10.4 ± 0.7	7	0.46 ± 0.27
	URA3-HOM3	435	767	44	1246	41.4 ± 1.6	127	0.35 ± 0.07
	HIS1-TRP2	982	214	2	1198	9.4 ± 0.7	5	0.37 ± 0.26
gmc2Δ	*CAN1-URA3*	547	666	15	1228	30.8 ± 1.1	81	0.19 ± 0.05
	URA3-HIS1	514	653	39	1206	36.8 ± 1.6	79	0.50 ± 0.09
	HIS1-HOM3	1160	29	0	1189	0.6 ± 0.16	0.09	N.A.
	HOM3-TRP2	855	302	14	1171	16.5 ± 1.1	12	1.17 ± 0.34*
	URA3-HOM3	533	647	33	1213	34.8 ± 1.5	59	0.44 ± 0.09
	HIS1-TRP2	877	277	10	1164	14.5 ± 1.0	10	1.00 ± 0.34*

Map distances and NPD ratios were calculated as described in the Material and Methods.

[a] PD: parental di-type, TT:tetra type, NPD: non-parental di-type.

[b] The SE for the map distances and NPD ratio with SE were calculated using the Stahl Lab online tool (https://elizabethhousworth.com/StahlLabOnlineTools/).

[c] Papazian analysis cannot be applied when the frequency of TTs exceeds 2/3 of the total.

* The significance of the difference in MAP distance and NPD ratio between the wild type and the mutant were confirmed by overlap of the SE value around the map distance or NPD ratio. N.A.: not applicable.

Supplementary table 3. Non-Mendelian segregation frequencies on chromosomes III and VII.

Isogenic SK1 strain	Chromosome III				Chromosome VII					Total No. of tetrad
	URA3	*LEU2*	*HIS4*	*MAT*	*CUP2*	*MET13*	*CYH2*	*TRP5*	*ADE6*	
Wild type	1.7 (1.0)	6.2 (1.0)	1.5 (1.0)	1.0 (1.0)	5.4 (1.0)	5.1 (1.0)	0.94 (1.0)	1.4 (1.0)	2.6 (1.0)	1381
gmc2Δ	1.3 (0.76)	6.6 (1.1)	1.9 (0.9)	1.7 (1.3)	13.0 (1.2)	7.8 (1.1)	4.7 (0.9)	2.6 (1.1)	7.1 (1.7)	1159
P-value [a]	0.63	0.68	0.54	0.16	1.6 x e^{-11}	0.007	4.3 x e^{-9}	0.039	8.1 x e^{-7}	

Congenic SK1 strain	Chromosome V					III	VII	Total No. of tetrad
	CAN1	*URA3*	*HIS1*	*HOM3*	*TRP2*	*MAT*	*CYH2*	
Wild type	0.7 (1.0)	0.1 (1.0)	2.0 (1.0)	0.8 (1.0)	2.7 (1.0)	0.6 (1.0)	0.6 (1.0)	1257
gmc2Δ	0.8 (1.1)	0.4 (5.1)	2.5 (1.3)	1.9 (2.4)	3.9 (1.4)	1.0 (1.7)	1.6 (2.9)	1242
P-value [a]	0.98	0.10	0.39	0.95	0.10	0.24	0.01	

Percentages of tetrad-type with 3+:1–, 1+:3–, 4+:0–, and 0+:4– segregation for each marker were shown. The ratios of the frequency in the mutant relative to that in the wild type are shown in parentheses.

[a] The statistical significance of the differences between the wild type and the *gmc2Δ* was calculated using Chi-square test.